New 3D Analytical Solution for Modeling Transient Unsaturated Flow Due to Wetting and Drying

André Luís Brasil Cavalcante, Ph.D.[1]; Lucas Parreira de Faria Borges[2]; and Jorge Gabriel Zornberg, Ph.D.[3]

Abstract: This study presents a novel three-dimensional (3D) analytical solution to the Richards equation, which takes as a basis a linear unsaturated model that was previously proposed. Specifically, the partial differential equation governing the transient, unsaturated flow phenomenon could be solved when using specific constitutive hydraulic functions that linearize the problem. The new 3D analytical solution could also be simplified to two-dimensional (2D) and one-dimensional (1D) analytical solutions, which make possible the evaluation of water flow using the constraints relevant for field and experimental settings. Two general cases of transient moisture movement are simulated using the new analytical solutions. The first case involves a wetting process, in which the flow within the soil mass is triggered by the initial presence of a specific region within the domain that had been subjected to an increased volumetric water content (e.g., because of precipitation or irrigation). In this case, water flows under unsaturated conditions from the region of increased moisture to the surrounding soil mass. The second case involves the recovery of an unconfined soil mass (e.g., an aquifer) within which a limited region had been subjected to a decreased volumetric water content (e.g., because of a localized drying process). In this case, water flow occurs from the soil mass into the region characterized by an initially low moisture content. The solutions presented in the study can be implemented to address a broad range of applications, providing insight into the complex phenomenon of soil wetting and drying. In particular, the solutions highlight the relative impact of the advective and diffusive components of unsaturated flow processes in multidimensional transient problems. **DOI: 10.1061/(ASCE)GM.1943-5622.0001461.**

Author keywords: Unsaturated flow; Transient flow; Wetting; Drying.

Introduction

The Richards equation is a relevant mathematical expression in soil mechanics that governs the migration of moisture within porous media, such as soil, under unsaturated conditions. Solutions to the Richards equation can be particularly relevant in geotechnical and geoenvironmental engineering applications involving unsaturated soils. Several numerical solutions to the Richards equation have been proposed in the technical literature to solve problems involving transient unsaturated water flow (Wang and Dooge 1994; Basha 1999; Chen et al. 2003). However, mainly because of the highly nonlinear form of the equation, only a few analytical solutions were available (Warrick et al. 1991; Massabó et al. 2011; Chen and Liu 2011; Ozelim and Cavalcante 2013; Guerrero et al. 2013; De Luca and Cepeda 2016; Bharati et al. 2017) to address problems with comparatively simple boundary and initial conditions.

Because of the difficulty in finding analytical solutions, unsaturated transient problems involving water flow within a soil mass have been solved using numerical schemes in most cases. Although feasible, the use of numerical approaches may entail high computational costs as well as possible mathematical errors in the numerical predictions. In addition, numerical approaches require initial benchmarking using closed-form analytical solutions to assess their adequacy.

Cavalcante and Zornberg (2017a) proposed a formulation of the Richards equation that resulted in a closed-form solution after identifying specific constitutive models that are capable of linearizing the conservation equation. In particular, it became possible to find analytical transient solutions, which proved particularly useful to conduct parametric evaluations and to validate the accuracy of numerical schemes.

The one-dimensional (1D) analytical and numerical solutions obtained by Cavalcante and Zornberg (2017a, b) provided the initial analytical framework for further analytical developments. Accordingly, the present paper proposes three-dimensional (3D) analytical solutions to the Richards equation that are capable of describing both the wetting and drying processes within an unsaturated soil mass. The solutions presented in this paper are expected to be particularly relevant for applications seeking minimal computational effort to solve comparatively complex transient problems.

A commonly used 3D form of the Richards equation can be expressed as

$$\frac{\partial \theta}{\partial t} = \frac{\partial}{\partial x}\left[\frac{k_x(\psi)}{\rho_w g}\frac{\partial \psi}{\partial x}\right] + \frac{\partial}{\partial y}\left[\frac{k_y(\psi)}{\rho_w g}\frac{\partial \psi}{\partial y}\right] + \frac{\partial}{\partial z}\left[k_z(\psi)\left(\frac{1}{\rho_w g}\frac{\partial \psi}{\partial x} - 1\right)\right] \quad (1)$$

where θ = volumetric water content of the soil [$L^{-3}L^3$]; k_x, k_y, and k_z = soil unsaturated hydraulic conductivity in the x-, y-, and

[1]Associate Professor, Dept. of Civil and Environmental Engineering, Univ. of Brasília, Brasília-DF 70910-900, Brazil (corresponding author). ORCID: https://orcid.org/0000-0003-4980-1450. Email: abrasil@unb.br

[2]Ph.D. Candidate, Dept. of Civil and Environmental Engineering, Univ. of Brasília, Brasília-DF 70910-900, Brazil. Email: lucaspdfborges@gmail.com

[3]Professor, Dept. of Civil, Architectural and Environmental Engineering, Univ. of Texas at Austin, Austin, TX 78712-0280. ORCID: https://orcid.org/0000-0002-6307-1047. Email: zornberg@mail.utexas.edu

Note. This manuscript was submitted on May 14, 2018; approved on January 29, 2019; published online on May 9, 2019. Discussion period open until October 9, 2019; separate discussions must be submitted for individual papers. This paper is part of the ***International Journal of Geomechanics***, © ASCE, ISSN 1532-3641.

z-directions [LT^{-1}], respectively; ψ = soil suction [$M\,L^2\,T^{-2}$]; ρ_w = water specific mass [ML^{-1}]; and g = acceleration of gravity [$L\,T^{-2}$].

The unsaturated hydraulic conductivity along a single dimension is considered to vary with suction according to the following expression (Cavalcante and Zornberg 2017a):

$$k(\psi) = k_s e^{-\delta\psi} \tag{2}$$

where k_s = soil saturated hydraulic conductivity; and δ = fitting hydraulic parameter [$M^{-1}LT^2$]. As described by Cavalcante and Zornberg (2017a), the "delta" is a parameter that defines the shape of the soil–water retention curve (SWRC) (it is proportional to its initial slope) and of the K function (it is also proportional to its initial slope). Also, considering the model proposed by Cavalcante and Zornberg (2017a), the soil suction is assumed to vary with the soil volumetric water content as follows:

$$\psi(\theta) = -\frac{1}{\delta}\ln\left(\frac{\theta - \theta_r}{\theta_s - \theta_r}\right) \tag{3}$$

where θ = volumetric water content of the soil [$L^{-3}L^3$]; θ_s = saturated volumetric water content of the soil [$L^{-3}L^3$]; and θ_r = residual volumetric water content of the soil [$L^{-3}L^3$]. In the literature, one can find descriptions of SWRCs with more complex models that allow a physical description of soil properties with the least amount of effort. Some of the commonly used analytical models of SWRC in the literature are the Gardner (1958), Brooks and Corey (1964), van Genuchten (1980), and Fredlund and Xing (1994) models. In addition, models, such as Arairo et al (2012), can also represent hysteretic scanning curves. Using the hydraulic functions defined by Eqs. (2) and (3), Cavalcante and Zornberg (2017a) could linearize the Richards equation, which in its complete dimensional form can be expressed as

$$\frac{\partial\theta}{\partial t} = \bar{D}_x\frac{\partial^2\theta}{\partial x^2} + \bar{D}_y\frac{\partial^2\theta}{\partial y^2} + \bar{D}_z\frac{\partial^2\theta}{\partial z^2} - \bar{a}_s\frac{\partial\theta}{\partial z} \tag{4}$$

with

$$\bar{D}_x = \frac{k_{sx}}{\rho_w g(\theta_s - \theta_r)\delta} \tag{5}$$

$$\bar{D}_y = \frac{k_{sy}}{\rho_w g(\theta_s - \theta_r)\delta} \tag{6}$$

$$\bar{D}_z = \frac{k_{sz}}{\rho_w g(\theta_s - \theta_r)\delta} \tag{7}$$

$$\bar{a}_s = \frac{k_{sz}}{(\theta_s - \theta_r)} \tag{8}$$

where k_{sx}, k_{sy}, and k_{sz} = soil saturated hydraulic conductivity in the x-, y-, and z-directions [LT^{-1}], respectively; $\bar{D}_x$, $\bar{D}_y$, and $\bar{D}_z$ = unsaturated water diffusivity values in the x-, y-, and z-directions [L^2T^{-1}], respectively; and $\bar{a}_s$ = unsaturated advective seepage [LT^{-1}].

Ultimately, the nonlinear Richards equation [Eq. (1)] could be formulated as Eq. (4), which corresponds to a linear, 3D partial differential equation (PDE). This formulation can be used to solve transient, unsaturated flow problems to predict the changes in volumetric water content within a soil through space and in time.

As a transient PDE, Eq. (4) defines the unsaturated flow phenomenon within a specific domain. In addition, its solution requires equations that govern the phenomenon within its boundaries and a third equation that defines the initial condition within the domain.

The equations that define the phenomenon within the domain must be established for each of the three dimensions of the problem. For the z-direction, a Dirichlet boundary condition was adopted, which involved a constant volumetric water content imposed at the upper and lower boundaries of the domain. The equations that define the boundary conditions of the problem under investigation are

$$\theta(x, y, 0, t) = \theta_0 \tag{9}$$

$$\theta(x, y, l_z, t) = \theta_0 \tag{10}$$

where l_z = depth of the domain from the ground surface, with $0 \le z \le l_z$, and $l_z \in \Re$, $\theta_0 \in \Re$.

For the x-direction, the boundary conditions, indicating an impermeable boundary, are

$$\lim_{x\to\infty}\frac{\partial\theta(x, y, z, t)}{\partial x} = 0 \tag{11}$$

$$\lim_{x\to-\infty}\frac{\partial\theta(x, y, z, t)}{\partial x} = 0 \tag{12}$$

where the range of x corresponds to $-\infty < x < \infty$.

For the y-direction, the boundary conditions also correspond to impermeable boundaries at infinitum, as follows:

$$\lim_{y\to\infty}\frac{\partial\theta(x, y, z, t)}{\partial y} = 0 \tag{13}$$

$$\lim_{y\to-\infty}\frac{\partial\theta(x, y, z, t)}{\partial y} = 0 \tag{14}$$

where the range of y corresponds to $-\infty < y < \infty$.

The equation adopted to define the initial condition in the problem under investigation can be mathematically expressed as

$$\begin{aligned}\theta(x,y,z,0) = (\theta_i - \theta_0)&\left[H(z) - H(z - b_z)\right]\\ &\times \left[H(y + b_y) - H(y - b_y)\right]\\ &\times \left[H(x + b_x) - H(x - b_x)\right] + \theta_0\end{aligned} \tag{15}$$

where b_x, b_y, and b_z = length in the x-, y-, and z-directions.

The function H in Eq. (15) corresponds to the Heaviside function, which is defined as

$$H(x) = \frac{1 + \mathrm{sgn}(x)}{2} \tag{16}$$

with

$$\mathrm{sgn}(x) = \begin{cases} -1, & \text{if } x < 0 \\ 0, & \text{if } x = 0 \\ 1, & \text{if } x > 0 \end{cases} \tag{17}$$

The initial condition can be represented as a cuboid within the domain with a volumetric moisture content different from that of the rest of the soil mass (Fig. 1). The volumetric water content within the box is θ_i, and that for the rest of the domain it is θ_0. The box may have a volumetric water content that is comparatively higher or lower than that in the rest of the surrounding soil mass. Thus, it is possible to simulate both drying and wetting processes, as will be discussed in the first and second simulations, respectively, for the 3D case evaluated in this study.

The solution of the transient unsaturated flow problem represented by Eq. (4), considering the boundary conditions represented by Eq. (9) to Eq. (14), and the initial conditions characterized by Eq. (15) could be solved using Fourier transforms. The explicit solution to this PDE was found to be

$$\theta(x,y,z,t) = \theta_0 + \frac{(\theta_i - \theta_0)}{4}\left[\operatorname{erf}\left(\frac{b_x - x}{\sqrt{4\pi\bar{D}_x t}}\right) + \operatorname{erf}\left(\frac{b_x + x}{\sqrt{4\pi\bar{D}_x t}}\right)\right]\left[\operatorname{erf}\left(\frac{b_y - y}{\sqrt{4\pi\bar{D}_y t}}\right) + \operatorname{erf}\left(\frac{b_y + y}{\sqrt{4\pi\bar{D}_y t}}\right)\right]$$
$$\times \sum_{n=1}^{\infty}\left\{\left[\frac{4\bar{D}_z e^{-\frac{\bar{a}_s b_z}{2\bar{D}_z}}\left(-2\pi\bar{D}_z n\, e^{\frac{\bar{a}_s b_z}{2\bar{D}_z}} + \bar{a}_s l_z \sin\left(\frac{\pi b_z n}{l_z}\right) + 2\pi\bar{D}_z n\cos\left(\frac{\pi b_z n}{l_z}\right)\right)}{\bar{a}_s^2 l_z^2 + 4\pi^2\bar{D}_z^2 n^2}\right]\right.$$
$$\left.\times\left[n\pi\cos\left(\frac{n\pi}{l_z}b_z\right) + \frac{l_z\bar{a}_s}{2\bar{D}_z}\sin\left(\frac{n\pi}{l_z}b_z\right)\right].\ \exp\left[-t\left(\frac{\bar{a}_s^2}{4\bar{D}_z} + \frac{\bar{D}_z n^2\pi^2}{l_z^2}\right)\right].\ \exp\left[\frac{\bar{a}_s z}{2\bar{D}_z}\right]\sin\left(\frac{n\pi}{l_z}z\right)\right\} \tag{18}$$

with

$$\operatorname{erf}(x) = \frac{2}{\sqrt{\pi}}\int_0^x e^{-t^2}dt \tag{19}$$

Details on the derivation of the solution represented by Eq. (18) are provided in the Appendix.

The analytical solution, originated on the unsaturated flow model, has a relevant whole on simulations. The solution is capable of estimating, with a high precision, the volumetric water content. Thus, it can be implemented on several applications of software that computes the water flow in a porous media. There is no doubt that the computational cost for processing an analytical solution is smaller than a numerical one. In addition, it is inherently more precise. Moreover, the analytical solution may be used to validate numerical simulations. In other words, it can be used as a reference to evaluate if a simulation was correctly run and if the numerical code was correctly implemented.

The solution of the PDE presented in the paper was implemented by the authors using Mathematica 11.3 using its functional programming language, Wolfram Mathematica.

Analytical Solution of 3D Transient, Unsaturated Flow Problems

Two cases of transient moisture movement are evaluated using the analytical solution to 3D problems represented by Eq. (18). The first

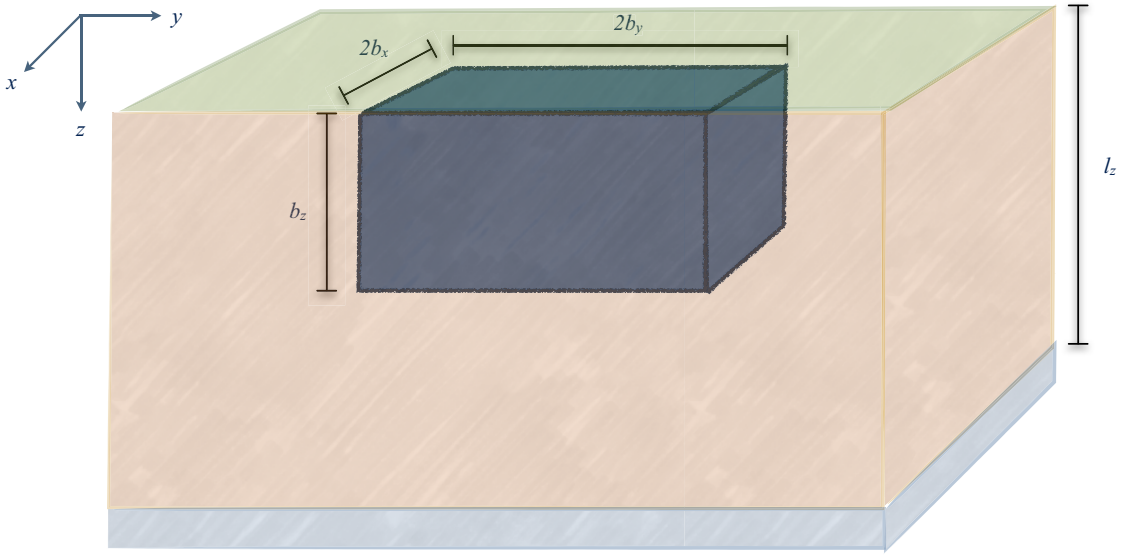

Fig. 1. Schematic representation of the initial condition.

case involves a wetting process, in which unsaturated flow is triggered by the presence of a cuboidal soil region with an initial volumetric water content that is higher than that in the rest of the domain. This case may correspond to a problem involving the local release of water (e.g., from precipitation, pipe leakage, irrigation) that resulted in a region within the soil mass characterized by a comparatively high initial volumetric moisture content in relation to that of the surrounding soil mass. In this case, water is expected to flow from the region of high moisture content to the surrounding soil mass. The second case involves unsaturated flow triggered by the presence of a cuboidal soil region with an initial volumetric water content that is lower than that in the rest of the domain. This case may correspond to the recovery of the recharge zone from an unconfined aquifer in which a region had been subjected to a localized drying process (e.g., caused by changes in vegetation or surface water management). In this case, water is expected to flow from the surrounding soil mass into the region characterized by low initial volumetric moisture content.

The hydraulic characteristics of the soil adopted in the two 3D problems are considered to be typical of sandy soils. Table 1 presents the soil hydraulic parameters adopted for the two cases evaluated in this study. The values were selected in Table 1 considering the orders of magnitude that correspond to sandy soils. Also, γ_w is the water unit weight.

Fig. 2 represents the unsaturated hydraulic function of the soil. For cases in which the soil is isotropic, only one unsaturated hydraulic conductivity function needs to be described.

Fig. 3 is a representation of the SWRC, which is the graphical form of Eq. (3). Only one SWRC is considered for the 3D problem illustrated in this study because the soils are assumed to be isotropic. Hysteresis was not considered in this study to simplify the mathematical solution, although the model is able to reproduce the hysteresis of the scanning curves, as presented by Arairo et al. (2012).

Table 1. Soil hydraulic parameters adopted in the illustrative analyses

Parameters of the illustrative analyses	Corresponding value
γ_w (kN/m^3)	9.8
δ	0.01
θ_s	0.61
k_{sx}, k_{sy}, k_{sz} (m/s)	10^{-6}
D_x, D_y, D_z (m^2/s)	1.7×10^{-5}
a_s (m/s)	1.67×10^{-6}

Case I: 3D Simulation of a Wetting Process

In the first 3D illustrative simulation presented in this study, the analytical solution involves the presence of a region with comparatively high volumetric water content, which triggers wetting of the rest of the soil mass. The initial condition defines this high-moisture region as a box with dimensions of 4 m in width and length, and 0.5 m in height, as seen in Fig. 4. The volumetric water content in this region is 0.50, whereas the rest of the domain has a volumetric water content of 0.10 (Table 2). The total thickness of the soil layer is 5 m.

It is possible to simulate the evolution of volumetric water content for several time periods using the parameters defined for Case I. Fig. 5 illustrates the changes in volumetric water content throughout the domain. Because the problem is symmetric in the x- and y-directions, the two-dimensional (2D) images presented in Figs. 5(a–d) illustrate the volumetric moisture content time history for either the $x = 0$ or the $y = 0$ planes.

Moisture from the initial box-shaped region can be observed to spread because of the diffusive nature of the phenomenon. However, as given in Fig. 5(d), the moisture contours become less rounded close to the lower boundary because of the limitation imposed by the finite thickness of the soil layer. Additionally, the center of the high-moisture region moves downward, which can be observed in the movement of the darker portion in the figure.

Case II: 3D Simulation of a Drying Process

In the second 3D illustrative simulation, the analytical solution involves the presence of a comparatively low volumetric water content, which triggers drainage out of the rest of the soil mass. The initial condition defines this low-moisture region as a box with dimensions of 8 m in width and 2 m in length and height (Fig. 6). The volumetric water content in this region is 0.10, whereas the rest of

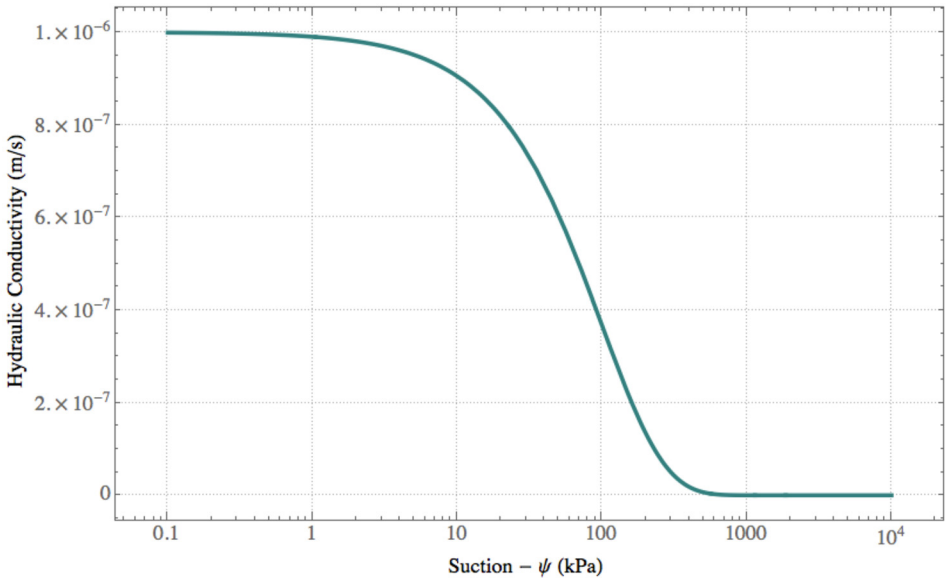

Fig. 2. Unsaturated hydraulic function of the soil.

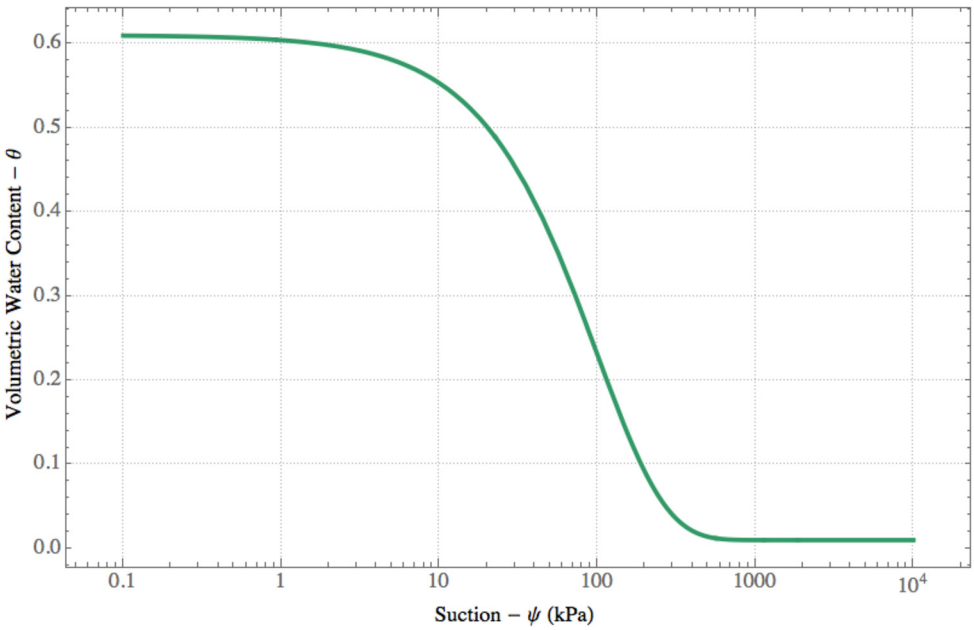

Fig. 3. SWRC.

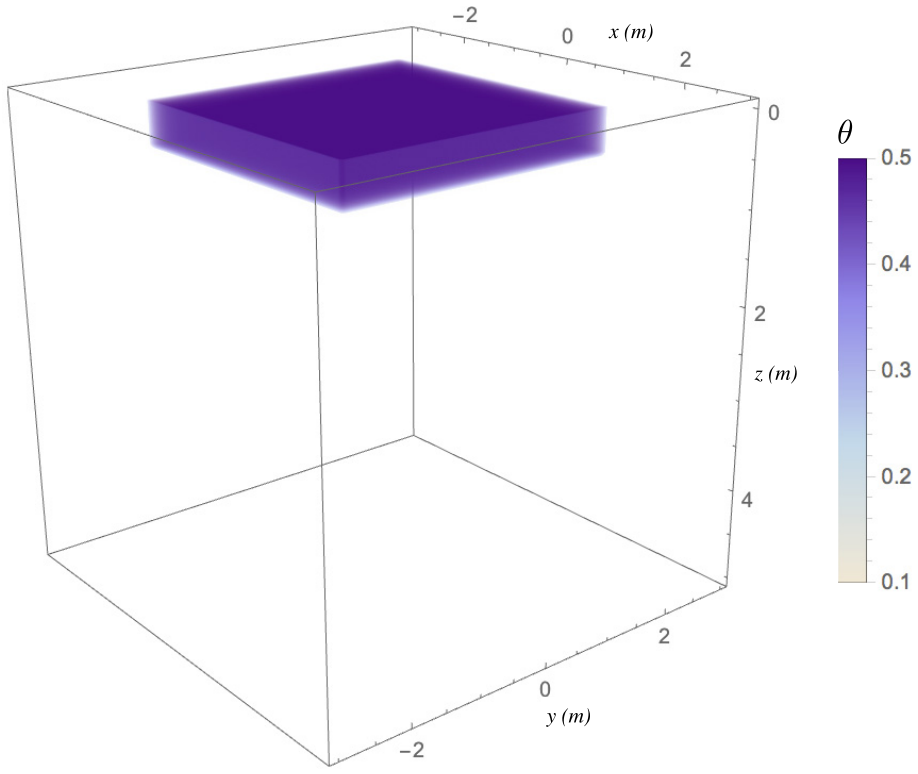

Fig. 4. Initial condition for the 3D Case I (wetting process).

the domain has a volumetric water content of 0.50 (Table 3). The total thickness of the soil layer is 5 m.

Fig. 7 illustrates the changes in volumetric water content throughout the domain, considering the volumetric moisture content time history for the $y = 0$ plane. On the other hand, Fig. 8 illustrates the time history for the $x = 0$ plane.

Consistent with the results predicted for Case I, the center of the low-moisture region moves downward, which can be observed in the movement of the lighter portion in Figs. 7 and 8. In this case, moisture from the region surrounding the initial box-shaped region migrates into this region because of the diffusive nature of the phenomenon, which results in the initially

rectangular dry region to evolve into a less spread out, ovoid region with time.

In terms of performance of the implemented solutions, a consistent physical answer to the problem was typically achieved using 100 terms in the series. Additional terms were found not to considerably add to the accuracy of the computed solutions. Although 3D simulations are often characterized by requiring significant computational cost, it took approximately 50 s to process the entire time-dependent 3D problem after running the code on a personal computer with reasonably simple hardware specifications [4-GB RAM and a 2.6-GHz dual core Intel central processing unit (CPU)]. As expected, however, the reported processing time would vary with the actual hardware used to conduct the simulations, with modern hardware and parallel processing anticipated to significantly reduce the processing time.

Table 2. Soil hydraulic parameters of Case I

Parameters used to simulate Case I	Corresponding value
θ_0	0.10
θ_i	0.50
b_x (m)	2
b_y (m)	2
b_z (m)	0.5
l_z (m)	5

Analytical Solution of 2D Transient, Unsaturated Flow Problems: 2D Simulation of an Anisotropic Process (Case III)

Cavalcante and Zornberg (2017a) proposed the linearization of the Richards equation, which is shown in its 3D form in Eq. (4). However, it is possible to simplify this formulation into a 2D form, as follows:

$$\frac{\partial \theta}{\partial t} = \bar{D}_x \frac{\partial^2 \theta}{\partial x^2} + \bar{D}_z \frac{\partial^2 \theta}{\partial z^2} - \bar{a}_s \frac{\partial \theta}{\partial z} \tag{20}$$

Only one step is needed to find the 2D solution considering the same boundary and initial conditions considered to obtain the 3D solution. Specifically, the limit should be obtained for the solution represented by Eq. (18) considering that b_y tends to infinity

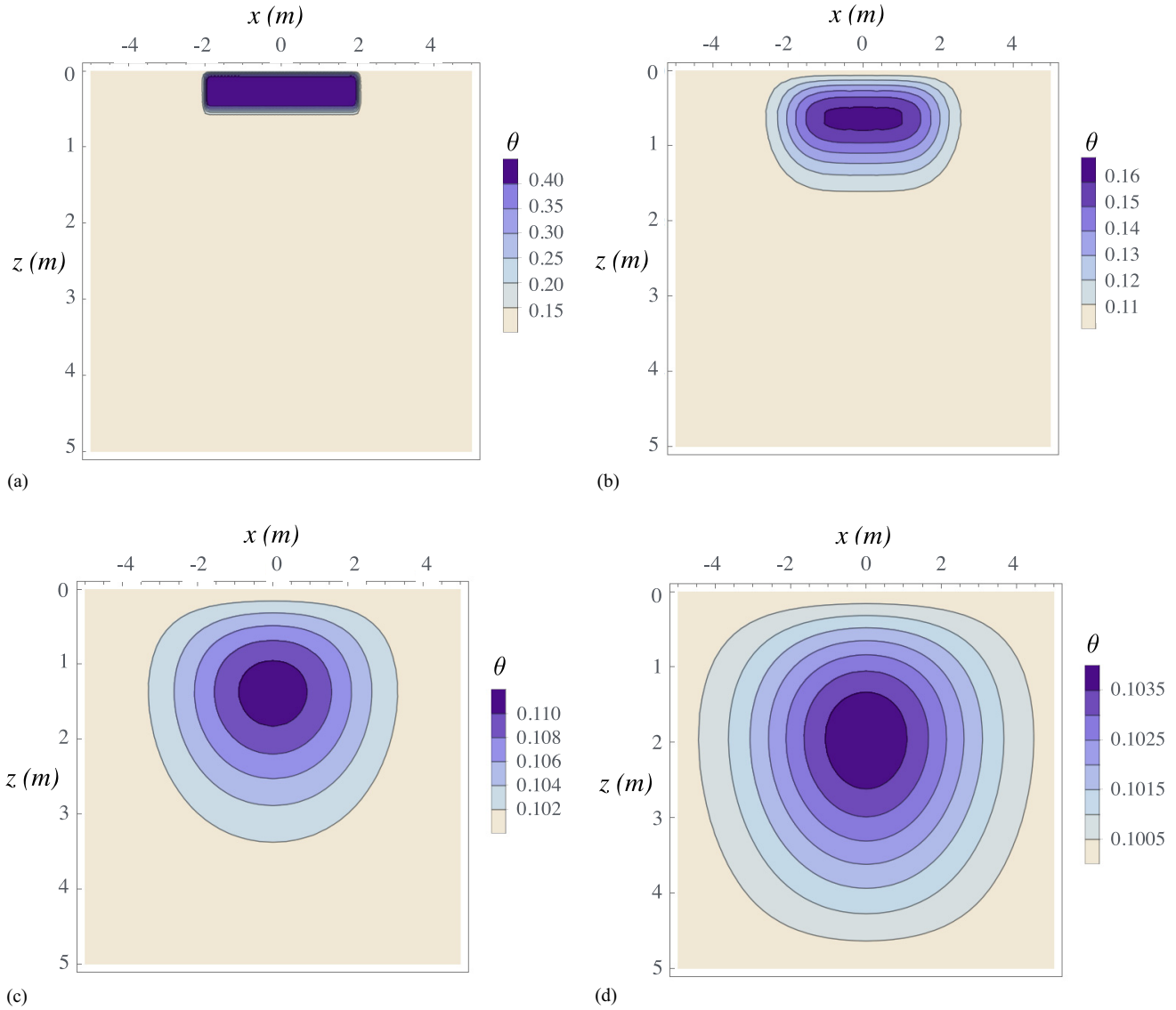

Fig. 5. Volumetric water content for the 3D wetting case for (a) $t = 100$ s; (b) $t = 10^4$ s; (c) $t = 5.10^4$ s; and (d) $t = 10^5$ s.

[Eq. (20)], which implies that the phenomenon leads to the same moisture content values for any value of y. That is

$$\lim_{b_y \to \infty} \theta(x, y, z, t) = \theta(x, z, t) \tag{21}$$

Therefore, the solution corresponds to that obtained for a single value of y. In this case, the solution can be represented in the x, z-plane as

$$\theta(x,z,t) = \theta_0 + \frac{(\theta_i - \theta_0)}{2}\left[\operatorname{erf}\left(\frac{b_x - x}{\sqrt{4\pi \bar{D}_x t}}\right) + \operatorname{erf}\left(\frac{b_x + x}{\sqrt{4\pi \bar{D}_x t}}\right)\right] \times \sum_{n=1}^{\infty}\left\{\left[\frac{4\bar{D}_z e^{-\frac{\bar{a}_s b_z}{2\bar{D}_z}}\left(-2\pi \bar{D}_z n\, e^{\frac{\bar{a}_s b_z}{2\bar{D}_z}} + \bar{a}_s l_z \sin\left(\frac{\pi b_z n}{l_z}\right) + 2\pi \bar{D}_z n \cos\left(\frac{\pi b_z n}{l_z}\right)\right)}{\bar{a}_s^2 l_z^2 + 4\pi^2 \bar{D}_z^2 n^2}\right] \times \left[n\pi \cos\left(\frac{n\pi}{l_z} b_z\right) + \frac{l_z a_s}{2 D_z} \sin\left(\frac{n\pi}{l_z} b_z\right)\right] \exp\left[-t\left(\frac{a_s^2}{4 D_z} + \frac{D_z n^2 \pi^2}{l_z^2}\right)\right] \exp\left[\frac{\bar{a}_s z}{2\bar{D}_z}\right] \sin\left(\frac{n\pi}{l_z} z\right)\right\} \tag{22}$$

The 2D simulation presented in this study involves using the previously developed solution to analyze a 2D section of the 3D solution. However, the opportunity is taken in this case to illustrate a case involving anisotropic conditions. Accordingly, the hydraulic properties Case III are different in the x- and z-directions. Specifically, the unsaturated hydraulic conductivity functions considered in this case in the x- and z-directions are those listed in Table 4 and illustrated in Figs. 9 and 10, respectively. The SWRC is assumed to be the same as that adopted in the 3D problems.

As presented in Table 4, the saturated hydraulic conductivity is 10 times bigger in the z-direction than that in the x-direction. Table 5 presents other parameters adopted for the simulation of Case III.

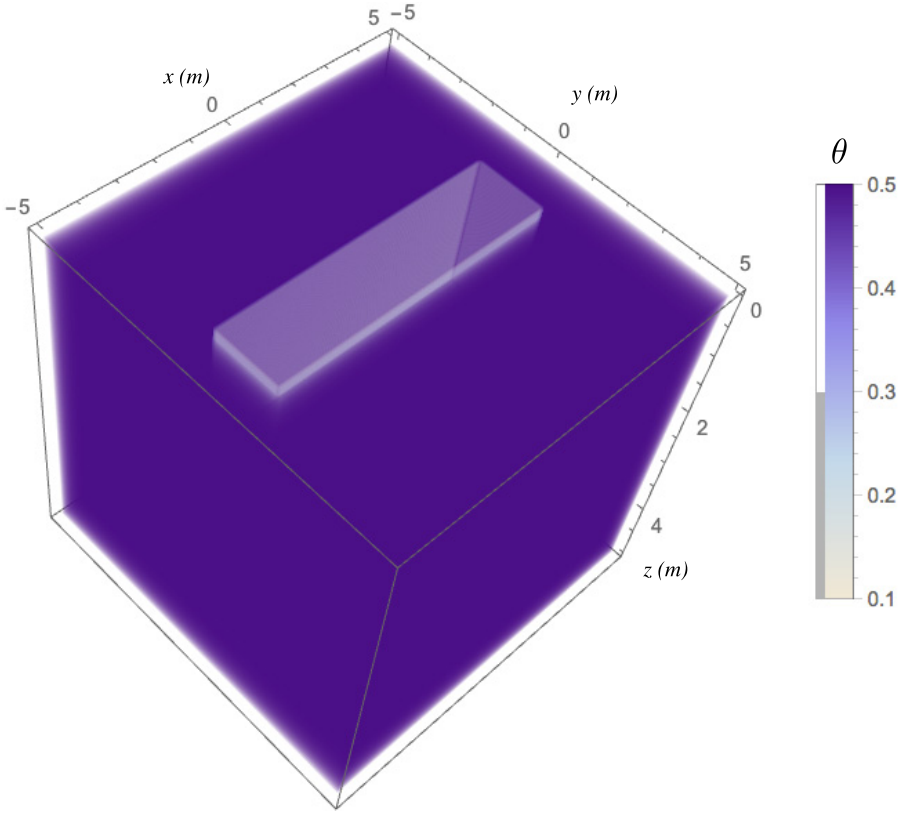

Fig. 6. Initial condition of 3D Case II.

Fig. 11(a) illustrates the initial condition for Case III, whereas Figs. 11(b–d) illustrate the volumetric moisture content time history for the solution of this problem.

As illustrated by the predictions given in Fig. 11, the higher hydraulic conductivity in the x-direction leads to greater moisture spread in the horizontal direction. On the other hand, the spread of moisture in the vertical direction is shown to be comparatively less significant.

Table 3. Soil hydraulic parameters of Case II

Parameters used to simulate Case II	Corresponding value
θ_0	0.50
θ_i	0.10
b_x (m)	4
b_y (m)	1
b_z (m)	2
l_z (m)	5

Analytical Solution of 1D Transient, Unsaturated Flow Problems: 1D Simulation (Case IV)

As with the considerations made to obtain the 2D solution as a special case of the 3D one, it is possible to further simplify the 2D solution to obtain a 1D solution. Although 1D solutions can be obtained in either the x-direction or the z-direction, the solution is presented in this study for the case of the 1D problem in the z-direction because it is relevant to represent important infiltration phenomena. Thus, for the case in which b_x tends to infinity, as follows:

$$\lim_{b_x \to \infty} \theta(x, z, t) = \theta(z, t) \tag{23}$$

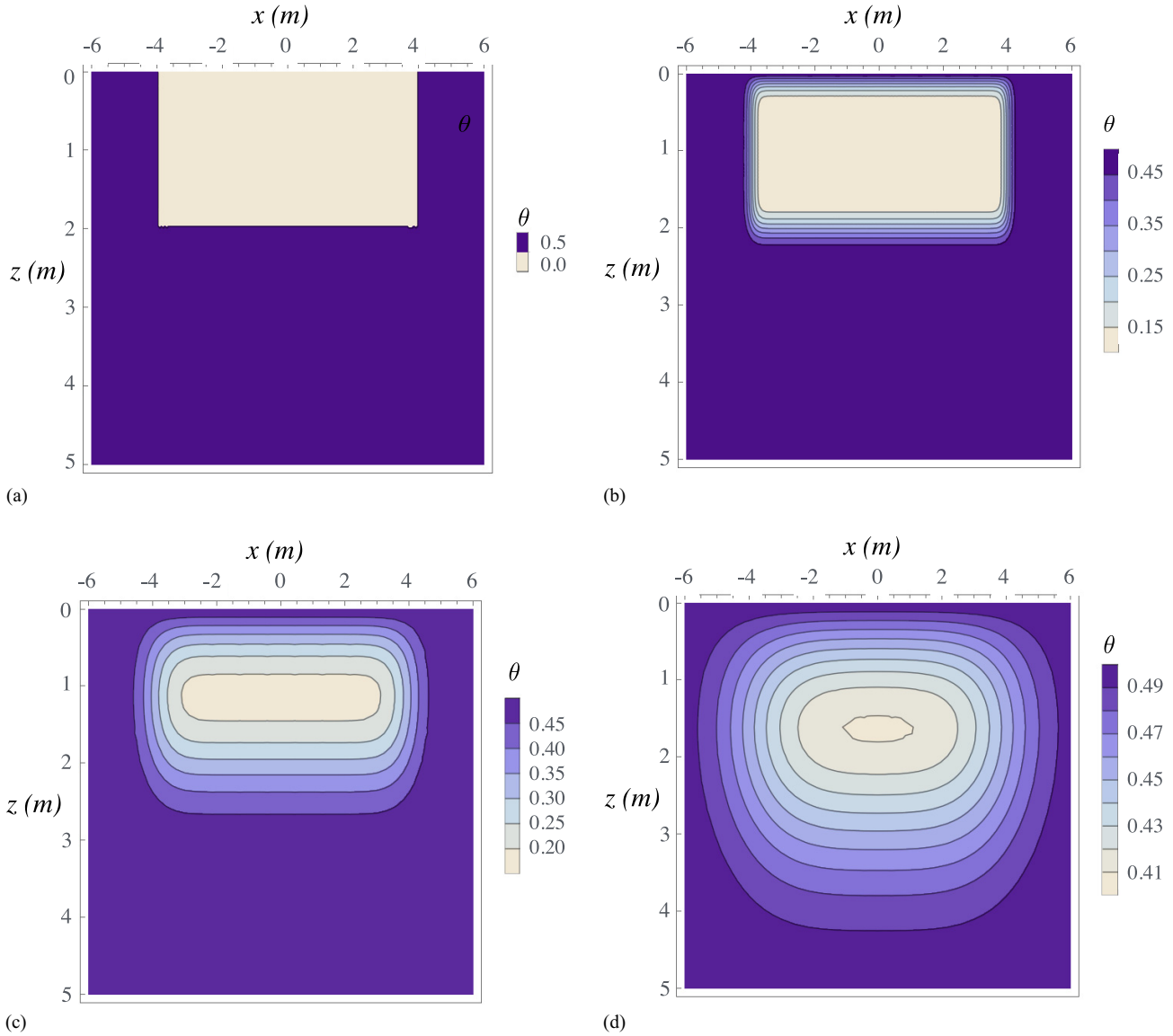

Fig. 7. Volumetric water content for the 3D drying case (plane $y = 0$) for (a) $t = 0$; (b) $t = 10^3$ s; (c) $t = 10^4$ s; and (d) $t = 5.10^4$ s.

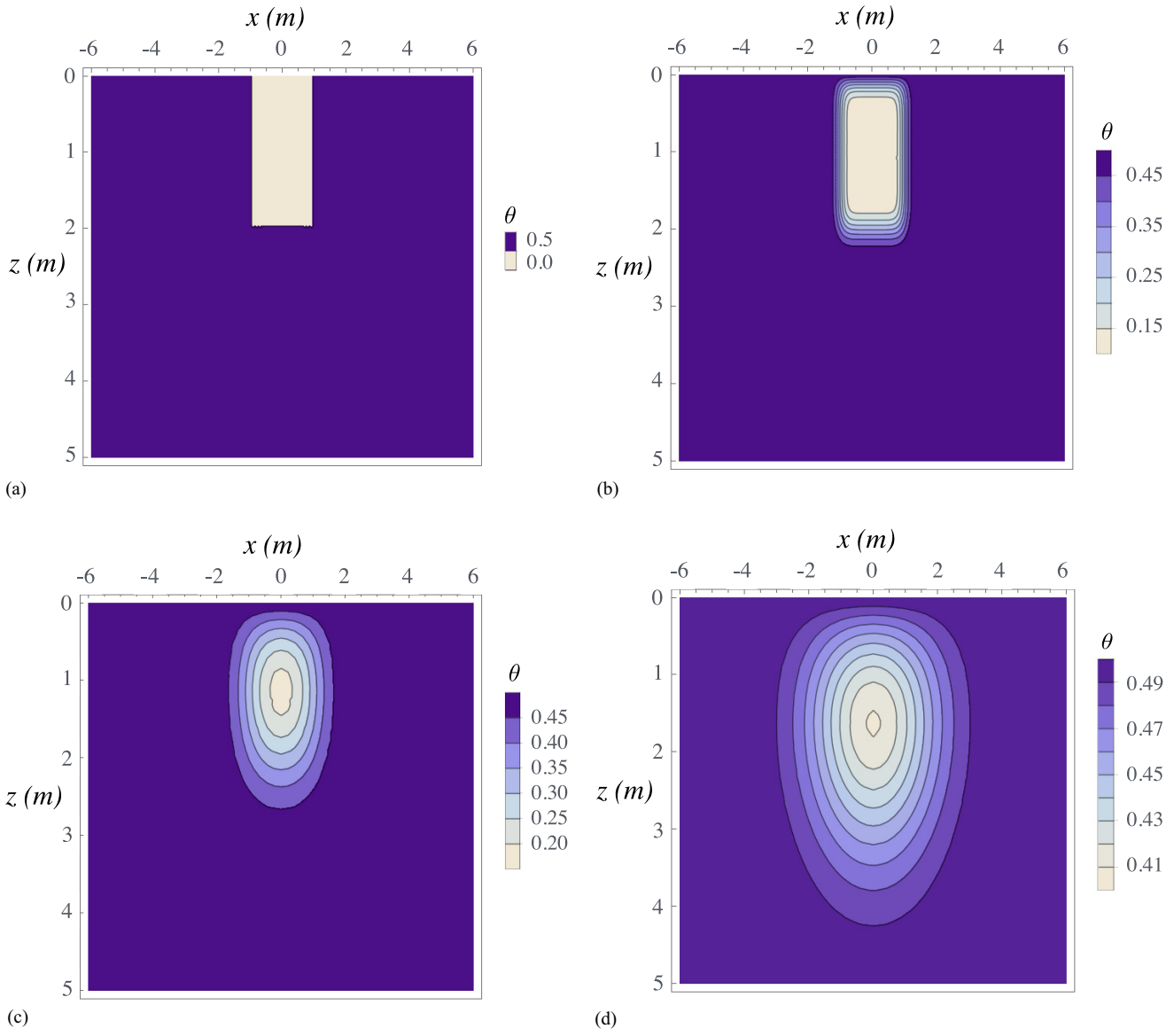

Fig. 8. Volumetric water content for the 3D drying case (plane $x = 0$) for (a) $t = 0$ s; (b) $t = 10^3$ s; (c) $t = 10^4$ s; and (d) $t = 5.10^4$ s.

The solution represented by Eq. (21) for a case in which b_x tends to infinity corresponds to that obtained for a single value of x. In this case, the solution can be represented along the z-axis as follows:

$$\theta(z,t) = \theta_0 + (\theta_i - \theta_0) \times \sum_{n=1}^{\infty} \left\{ \left[\frac{4\bar{D}_z e^{-\frac{\bar{a}_s b_z}{2\bar{D}_z}} \left(-2\pi\bar{D}_z n\, e^{\frac{\bar{a}_s b_z}{2\bar{D}_z}} + \bar{a}_s l_z \sin\left(\frac{\pi b_z n}{l_z}\right) + 2\pi\bar{D}_z n \cos\left(\frac{\pi b_z n}{l_z}\right) \right)}{\bar{a}_s^2 l_z^2 + 4\pi^2 \bar{D}_z^2 n^2} \right] \times \left[n\pi \cos\left(\frac{n\pi}{l_z} b_z\right) + \frac{l_z a_s}{2 D_z} \sin\left(\frac{n\pi}{l_z} b_z\right) \right] \exp\left[-t \left(\frac{a_s^2}{4D_z} + \frac{D_z n^2 \pi^2}{l_z^2} \right) \right] \exp\left[\frac{\bar{a}_s z}{2\bar{D}_z} \right] \sin\left(\frac{n\pi}{l_z} z\right) \right\} \tag{24}$$

Case IV illustrates the use of the previously developed solution for a 1D problem, similarly as previously done for the 2D and 3D solutions. In this simulation, the unsaturated water flow in the vertical direction is represented using the same unsaturated hydraulic conductivity function and water retention curve as those used in the 3D case for the z-direction (Table 1 and Figs. 2 and 3). The time

history of the soil volumetric water content is given in Fig. 12, in which the initial condition is presented in Fig. 12(a).

Although it is mathematically unnecessary to do so, both the x- and z-axes are represented in Fig. 12 to highlight the difference between the 1D solution shown in this figure and the 3D solution presented in Fig. 5.

Table 4. Constitutive model parameters of the 2D simulation

Constitutive parameters used in the 2D simulation	Corresponding value
δ	0.01
k_{sx} (m/s)	10^{-6}
k_{sz} (m/s)	10^{-7}

When comparing the 3D and 1D solutions, it can be observed that the maximum water volumetric content and the depth of the zone with this maximum value (in the z-direction) are essentially the same in the two solutions. On the other hand, the differences can be obviously noted in the other directions. Also, the 1D solution highlights the asymmetric nature of the unsaturated flow. Specifically, the results in Fig. 12 illustrate that the gradient of moisture content in the vertical direction, at a given time, is comparatively higher above the region of maximum volumetric water content than below this region. This is consistent with the nature of unsaturated flow, as described by the Richards equation. In other words, the gravity-driven advective flow component plays a relevant whole moving the water in the downward direction.

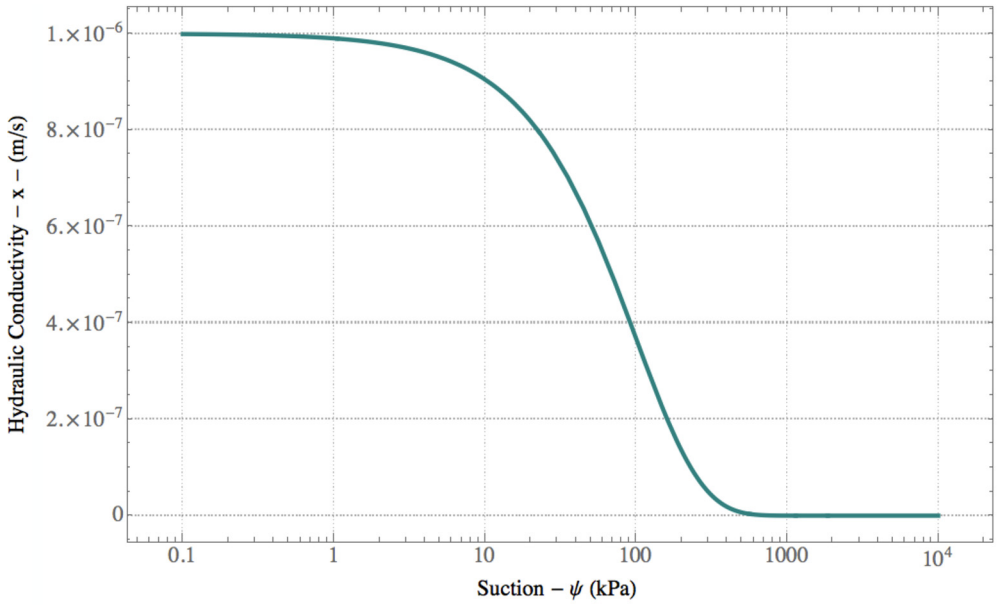

Fig. 9. Unsaturated hydraulic function in x for the 2D problem (Case III).

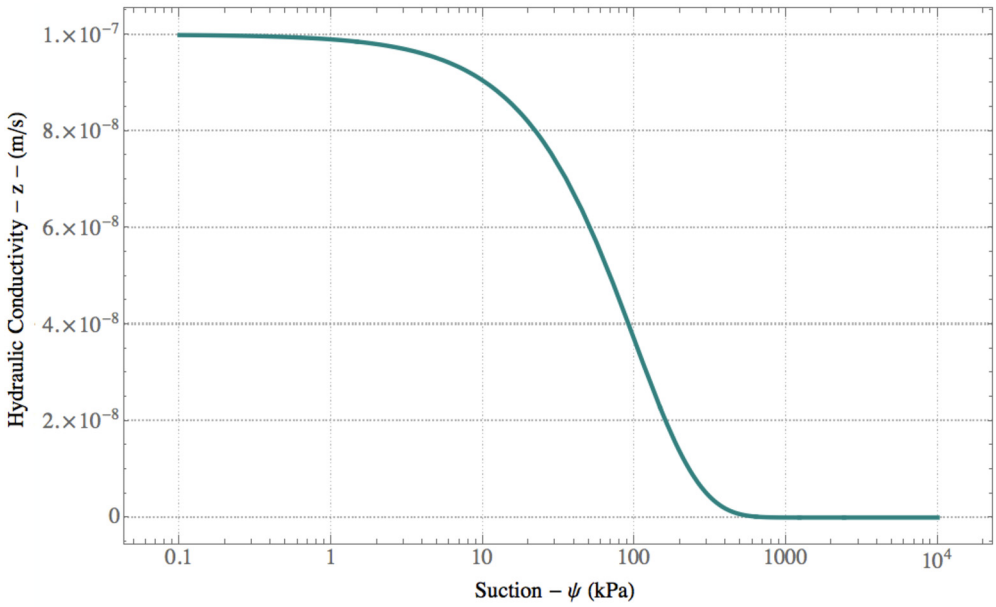

Fig. 10. Unsaturated hydraulic function in z for the 2D problem (Case III).

Conclusions

In this study, the analytical solutions were obtained for 3D transient problems involving unsaturated flow into or out of a region with comparatively higher or lower initial volumetric moisture content than the rest of the domain. Determination of the analytical solution was possible after adopting the models proposed by Cavalcante and Zornberg (2017a) for the SWRC and the hydraulic conductivity function. Specifically, selection of these hydraulic functions along with inverse Fourier transforms allowed the determination of the exact solution to the problem.

The obtained analytical formulation represents an exact and explicit solution, which eliminates the propagation of errors caused by discretization as well as problems associated with stability and convergence of numerical solutions. The analytical solution is expected to be particularly helpful in parametric evaluation studies as well as in validation of numerical simulations conducted for more complex boundary conditions and hydraulic functions.

The 3D solution could be simplified into 2D and 1D solutions. A number of cases were provided to illustrate the type of problems that could be addressed using the new analytical solution. They highlight the impact of the advective and diffusive components of the Richards equation in transient unsaturated flow problems.

Ultimately, the analytical expression developed in this study provides an efficient solution with a required computational effort significantly smaller than that required by numerical solutions. This is expected to facilitate the use of unsaturated flow concepts in both geotechnical research and engineering practice.

Table 5. Soil hydraulic parameters of the 2D simulation

Soil hydraulic parameters of the 2D simulation	Corresponding value
θ_0	0.10
θ_i	0.50
b_x (m)	0.5
b_z (m)	2
l_z (m)	5

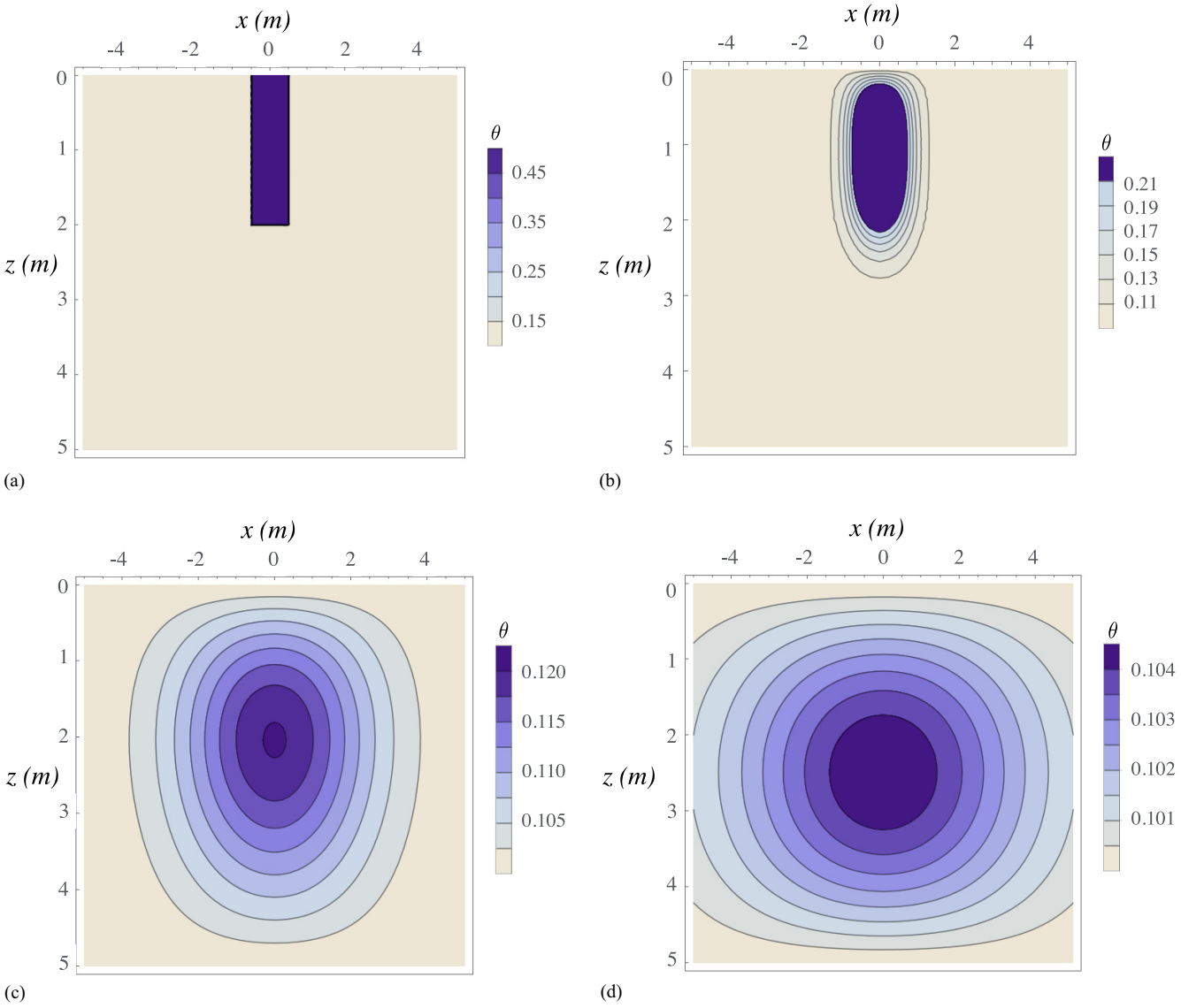

Fig. 11. Volumetric water content for the anisotropic 2D case for (a) $t = 0$; (b) $t = 5.10^3$ s; (c) $t = 10^5$ s; and (d) $t = 2.5\ 10^6$ s.

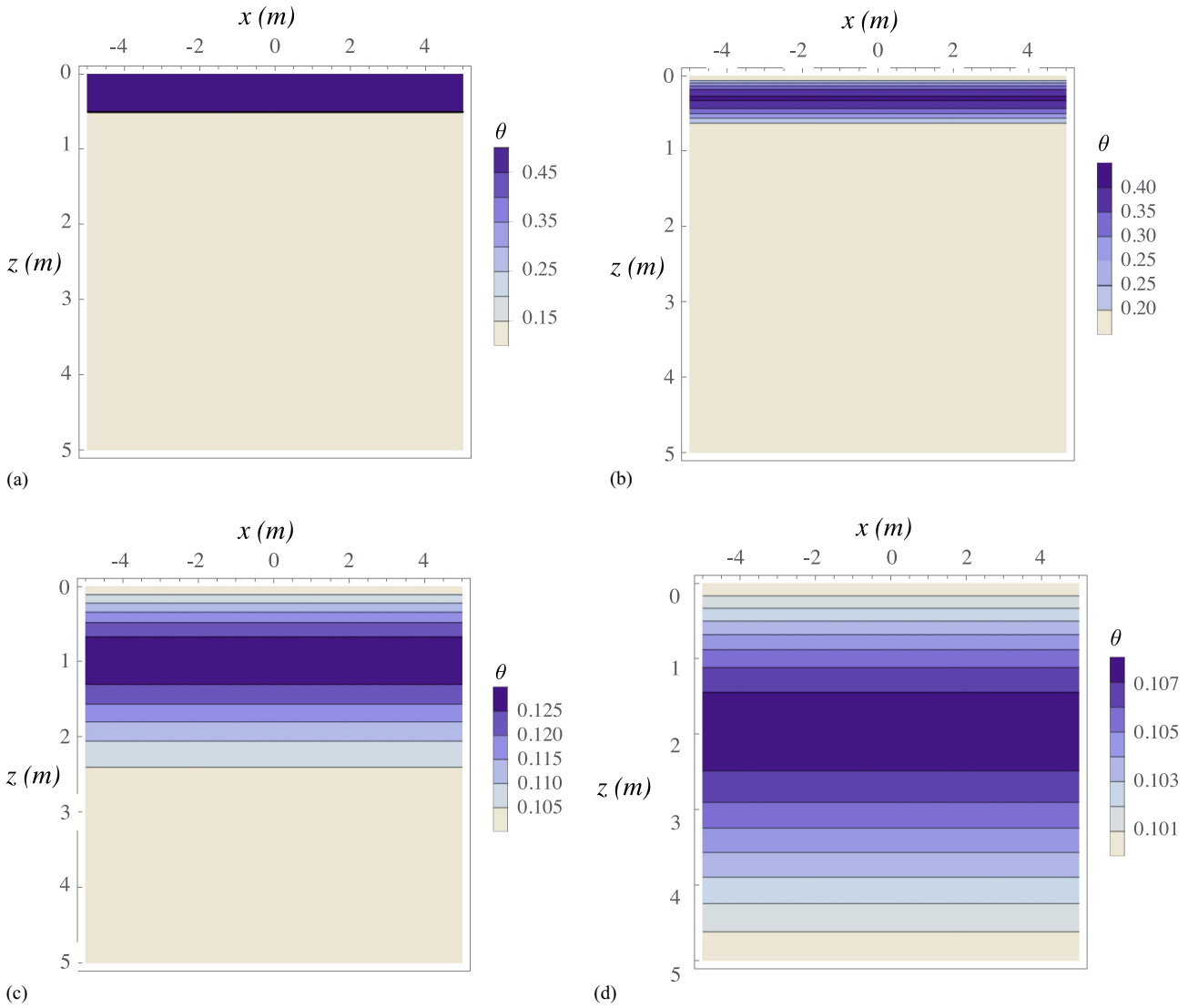

Fig. 12. Volumetric water content for (a) $t = 0$; (b) $t = 10^3$ s; (c) $t = 25.10^3$ s; and (d) $t = 10^5$ s.

Appendix. PROBLEM Solution

Separation of the Problem Separation

The problem must be separated into two distinct ones to find its solution. The first solution to be obtained is for the steady-state condition which, by definition, does not vary with time. The second problem involves obtaining the homogeneous solution, the boundaries of which have null values. The problem can be algebraically expressed as

$$\theta(x, y, z, t) = \theta_s(x, y, z, t) + \theta_h(x, y, z, t) \tag{25}$$

where $\theta_s(x, y, z, t)$ = steady-state solution and $\theta_h(x, y, z, t)$ is the homogeneous solution.

Steady-State Problem

The solution to steady-state problems, such as the one investigated in this study, can be a trivial one because the requirement is to find a solution that satisfies the boundary conditions and does not vary with time. Inspection of the boundary conditions reveals that the steady-state solution can be represented as

$$\theta_s(x, y, z, t) = \theta_0 \tag{26}$$

where θ_0 = moisture content at the boundary.

Homogeneous Problem

Once the steady-state solution has been identified, the homogeneous problem can be complementarily defined. The PDE that governs the main problem can be stated as the summation of each separate solution

$$\frac{\partial(\theta_s + \theta_h)}{\partial t} = \bar{D}_x \frac{\partial^2(\theta_s + \theta_h)}{\partial x^2} + \bar{D}_y \frac{\partial^2(\theta_s + \theta_h)}{\partial y^2} + \bar{D}_z \frac{\partial^2(\theta_s + \theta_h)}{\partial z^2} - \bar{a}_s \frac{\partial(\theta_s + \theta_h)}{\partial z} \tag{27}$$

However, because the solution to the steady-state problem is a constant, the PDE that governs the homogeneous problem can be defined as

$$\frac{\partial \theta_h}{\partial t} = \bar{D}_x \frac{\partial^2 \theta_h}{\partial x^2} + \bar{D}_y \frac{\partial^2 \theta_h}{\partial y^2} + \bar{D}_z \frac{\partial^2 \theta_h}{\partial z^2} - \bar{a}_s \frac{\partial \theta_h}{\partial z} \tag{28}$$

Also, considering the boundary conditions in the z-direction of the main problem, it is possible to verify that the boundary conditions for the homogeneous problem are null, that is

$$\theta_s(x, y, 0, t) + \theta_h(x, y, 0, t) = \theta_0 \tag{29}$$

$$\theta_h(x, y, 0, t) = 0 \tag{30}$$

$$\theta_h(x, y, 0, t) = 0 \tag{31}$$

$$\theta_s(x, y, l_z, t) + \theta_h(x, y, l_z, t) = \theta_0 \tag{32}$$

$$\theta_h(x, y, l_z, t) = 0 \tag{33}$$

Along the x-direction, it should also be satisfied that at its limit, the derivative tends to a null value, as follows:

$$\lim_{x \to \infty} \frac{\partial[\theta_s(x, y, z, t) + \theta_h(x, y, z, t)]}{\partial x} = 0 \tag{34}$$

$$\lim_{x \to \infty} \frac{\partial \theta_h(x, y, z, t)}{\partial x} = 0 \tag{35}$$

$$\lim_{x \to -\infty} \frac{\partial[\theta_s(x, y, z, t) + \theta_h(x, y, z, t)]}{\partial x} = 0 \tag{36}$$

$$\lim_{x \to -\infty} \frac{\partial \theta_h(x, y, z, t)}{\partial x} = 0 \tag{37}$$

As with the x-axis, the boundary conditions for the y-axis are also null

$$\lim_{y \to \infty} \frac{\partial \theta_h(x, y, z, t)}{\partial y} = 0 \tag{38}$$

$$\lim_{y \to -\infty} \frac{\partial \theta_h(x, y, z, t)}{\partial y} = 0 \tag{39}$$

Consequently, the initial condition of the homogeneous problem can be determined using the initial condition of the main problem minus the steady-state solution, as follows:

$$\theta_h(x, y, z, 0) = (\theta_i - \theta_0)\big[H(z) - H(z - b_z)\big][H(y + b_y) - H(y - b_y)][H(x + b_x) - H(x - b_x)] \tag{40}$$

Subdivisions on the Homogeneous Problem

The homogeneous solution can be stated as the product of three functions that have one spatial and temporal independent variable each

$$\theta_h(x, y, z, t) = f(x, t)k(y, t)g(z, t) \tag{41}$$

Therefore, substituting Eq. (41) into Eq. (4), the following formulation of the PDE is possible:

$$\frac{1}{f}\frac{\partial f}{\partial t} + \frac{1}{k}\frac{\partial k}{\partial t} + \frac{1}{g}\frac{\partial g}{\partial t} = \bar{D}_x \frac{\partial^2 f}{\partial x^2}\frac{1}{f} + \bar{D}_y \frac{\partial^2 k}{\partial x^2}\frac{1}{k} + \bar{D}_z \frac{\partial^2 g}{\partial z^2}\frac{1}{g} - \bar{a}_s \frac{\partial g}{\partial z}\frac{1}{g} \tag{42}$$

Solution for f (x,t)

Because all spatial variables (x, y, and z) have no mutual dependence, it is possible to split Eq. (42) into three PDEs. The first PDE depends on x and t alone, and it can be expressed as

$$\frac{\partial f(x, t)}{\partial t} = \bar{D}_x \frac{\partial^2 f(x, t)}{\partial x^2} \tag{43}$$

The boundary conditions of $f(x,t)$ can also be specified by combining Eqs. (11) and (12) with Eq. (41), as follows:

$$\lim_{x \to \infty} k(y, t)g(z, t) \frac{\partial f(x, t)}{\partial x} = 0 \tag{44}$$

Considering that $k(y,t)$ and $g(z,t)$ are not trivial solutions yields the following:

$$\lim_{x \to \infty} \frac{\partial f(x, t)}{\partial x} = 0 \tag{45}$$

The initial condition of $f(x,t)$ can also be obtained by combining Eqs. (40) and (41), as follows:

$$f(x, 0)k(y, 0)g(z, 0) = (\theta_i - \theta_0)[H(z) - H(z - b_z)][H(y + b_y) - H(y - b_y)][H(x + b_x) - H(x - b_x)] \tag{46}$$

It should be noted that the last factor of Eq. (46) is a function of x alone. All other factors, except for the first one, depend on other variables. Thus, the initial condition of $f(x,t)$ can be defined as

$$f(x, 0) = H(x + b_x) - H(x - b_x) \tag{47}$$

The Fourier transform (F) should be used to find a solution for $f(x,t)$. The Fourier transform is an integral transformation capable of mapping a region with boundaries in the infinitum. In this case, the variable x is mapped to the variable w, as follows:

$$\frac{\partial \widehat{f}(w, t)}{\partial t} = -w^2 \bar{D}_x \widehat{f}(w, t) \tag{48}$$

Considering the following:

$$\widehat{f}(w, t) = C(w)\, e^{\lambda t} \tag{49}$$

Eq. (48) can be rewritten as

$$\lambda\, C(w)\, e^{\lambda t} = -w^2 \bar{D}_x\, C(w)\, e^{\lambda t} \tag{50}$$

This implies that λ can be expressed as

$$\lambda = -w^2 \bar{D}_x \tag{51}$$

Therefore, $\widehat{f}(w, t)$ can be written as a combination of Eqs. (49) and (51)

$$\widehat{f}(w, t) = C(w)\, e^{-w^2 \bar{D}_x t} \tag{52}$$

It is known that $\widehat{f}(w,0)$ is the Fourier transform of $f(x,0)$

$$\widehat{f}(w,0) = \sqrt{\frac{2}{\pi}}\int_{-\infty}^{\infty} f(s,0)e^{iws}\,ds \tag{53}$$

Consequently, by combining Eqs. (49) and (53), the following expression for $C(w)$ can be obtained:

$$C(w) = \sqrt{\frac{2}{\pi}}\int_{-\infty}^{\infty} f(s,0)e^{iws}\,ds \tag{54}$$

Therefore, $\widehat{f}(w,t)$ can be expressed as a combination of Eqs. (49) and (54)

$$\widehat{f}(w,t) = \sqrt{\frac{2}{\pi}}\int_{-\infty}^{\infty} f(s,0)e^{iws}\,dse^{kt} \tag{55}$$

The following expressions can be reached by applying the inverse Fourier transform to Eq. (55):

$$\mathcal{F}^{-1}\left[\widehat{f}(w,t)\right] = \mathcal{F}^{-1}\left[\sqrt{\frac{2}{\pi}}\int_{-\infty}^{\infty} f(s,0)e^{iws}\,dse^{-w^2D_xt}\right] \tag{56}$$

Regarding integrals

$$f(x,t) = \sqrt{\frac{2}{\pi}}\int_{-\infty}^{\infty}\sqrt{\frac{2}{\pi}}\int_{-\infty}^{\infty} f(s,0)e^{iws}\,dse^{-w^2D_xt}\,e^{-iwx}\,dw \tag{57}$$

Separating the integrals from Eq. (57) yields the following:

$$f(x,t) = \frac{2}{\pi}\int_{-\infty}^{\infty} f(s,0)\left[\int_{-\infty}^{\infty} e^{-w^2D_xt}\,e^{iw(s-x)}\,dw\right]ds \tag{58}$$

Solving the last integral of Eq. (58) yields the following:

$$f(x,t) = \frac{\sqrt{\pi}}{\sqrt{4\pi}\sqrt{\bar{D}_x t}}\int_{-\infty}^{\infty} f(s,0)e^{\frac{-(s-x)^2}{4D_xt}}\,ds \tag{59}$$

By substituting the initial condition of Eq. (47) into Eq. (59), $f(x,t)$ can be modified to

$$f(x,t) = \frac{\sqrt{\pi}}{\sqrt{4\pi}\sqrt{\bar{D}_x t}}\int_{-\infty}^{\infty}[H(s+b_x) - H(s-b_x)]e^{\frac{-(s-x)^2}{4D_xt}}\,ds \tag{60}$$

Therefore, by solving the integral of Eq. (60), the solution of $f(x,t)$ can be found, which is expressed as

$$f(x,t) = \frac{1}{2}\left[\text{erf}\left(\frac{b_x - x}{\sqrt{4\pi\bar{D}_x t}}\right) + \text{erf}\left(\frac{b_x + x}{\sqrt{4\pi\bar{D}_x t}}\right)\right] \tag{61}$$

where erf is the error function, defined as

$$\text{erf}(x) = \frac{2}{\sqrt{\pi}}\int_0^x e^{-t^2}\,dt \tag{62}$$

Solution for k(y,t)

As previously stated, and because all spatial variables (x, y, and z) are not mutually dependent, Eq. (42) can be split into three PDEs. The second PDE depends on y and t alone, and it can be expressed as

$$\frac{\partial k(y,t)}{\partial t} = \bar{D}_y\frac{\partial^2 k(y,t)}{\partial y^2} \tag{63}$$

The boundary conditions of $k(y,t)$ can also be specified by combining Eqs. (13), (14), and (63) as

$$\lim_{y\to\infty} f(x,t)g(z,t)\frac{\partial k(y,t)}{\partial y} = 0 \tag{64}$$

Considering that $f(x,t)$ and $g(z,t)$ are not trivial solutions, it can be stated that

$$\lim_{y\to\infty}\frac{\partial k(y,t)}{\partial y} = 0 \tag{65}$$

Note that the third factor of Eq. (46) is a function of y alone. All other terms, except for the first, depend on other variables. Thus, the initial condition for $k(y,t)$ can be defined as

$$k(y,0) = H(y+b_y) - H(y-b_y) \tag{66}$$

It should be noted that all equations that define $f(x,t)$ are the same as those defining $k(y,t)$, but with f in place of k and x in place of y. Therefore, the same steps of the Fourier transform used to find $f(x,t)$ can be followed to find $k(y,t)$. Consequently, $k(y,t)$ can be expressed as

$$k(y,t) = \frac{1}{2}\left[\text{erf}\left(\frac{b_y - y}{\sqrt{4\pi\bar{D}_y t}}\right) + \text{erf}\left(\frac{b_y + y}{\sqrt{4\pi\bar{D}_y t}}\right)\right] \tag{67}$$

The third and last PDE that can be obtained from Eq. (42) depends only on z and t, and it is expressed as

$$\frac{\partial g(z,t)}{\partial t} = \bar{D}_z\frac{\partial^2 g(z,t)}{\partial z^2} - \bar{a}_s\frac{\partial g(z,t)}{\partial z} \tag{68}$$

Additionally, the boundary condition initially determined by Eq. (9) can be written as

$$f(x,t)k(y,t)g(0,t) = 0 \tag{69}$$

Knowing that f and k are nonnull functions, it is possible to express the initial condition as

$$g(0,t) = 0 \tag{70}$$

By combining Eqs. (10) and (41), it is also possible to define the other boundary condition, as

$$f(x,t)k(y,t)g(l_z,t) = 0 \tag{71}$$

As with the previously discussed boundary conditions, it is possible to state that the value of l_z is equal to

$$g(l_z,t) = 0 \tag{72}$$

All terms of Eq. (46) that do not depend on variables other than z determine the initial condition, as

$$g(z,0) = (\theta_i - \theta_0)\left[H(z) - H(z-b_z)\right] \tag{73}$$

Eq. (80) must be factorized into two independent functions to find the mathematical expression of $g(z,t)$, such as

$$g(z,t) = u(z)\,v(t) \tag{74}$$

Therefore, it is possible to describe the PDE represented by Eq. (68) using Eq. (74), and dividing by $u(z)\,v(t)$ yields the following:

$$\frac{v'(t)}{v(t)} = \bar{D}_z \frac{u''(z)}{u(z)} - \bar{a}_s \frac{u'(z)}{u(z)} \tag{75}$$

Solution for u(z)

Once u depends only on z, it is possible to restate Eq. (75) as

$$\bar{D}_z \frac{u''(z)}{u(z)} - \bar{a}_s \frac{u'(z)}{u(z)} = \lambda \tag{76}$$

Therefore, $u(z)$ can be generically described as

$$u(z) = c_1 e^{c_2 z}; \qquad c_1, c_2 \in \Re \tag{77}$$

Solving Eq. (77) yields the following:

$$\bar{D}_z c_2^2 - \bar{a}_s\, c_2 - \lambda = 0 \tag{78}$$

By isolating c_2 and considering that $\bar{a}_s^2 + 4\,\bar{D}_z\,\lambda < 0$, the following expression can be reached:

$$c_2 = k_1 \pm i\,k_2 \tag{79}$$

where

$$k_1 = \frac{\bar{a}_s}{2\,\bar{D}_z} \tag{80}$$

$$k_2 = \frac{\sqrt{|\bar{a}_s^2 + 4\bar{D}_z\,\lambda|}}{2\bar{D}_z} \tag{81}$$

Considering Eqs. (77) and (79), $u(z)$ can be described as

$$u(z) = a_1 e^{k_1 z} \sin(k_2\, z) + a_2 e^{k_1 z} \cos(k_2\, z) \tag{82}$$

Substituting $z = 0$ into Eq. (82) yields the following:

$$u(0) = a_1 \cdot 0 + a_2 \cdot 1 \tag{83}$$

Considering Eqs. (73) and (74), as well as that $h(t)$ is nonnull, it can be concluded that $g(0,t) = u(0)$. Consequently, it can be stated that

$$a_2 = 0 \tag{84}$$

Considering $z = l_z$ in Eq. (82) yields the following:

$$u(l_z) = a_1 e^{k_1 l_z} \sin(k_2\, l_z) \tag{85}$$

However, by combining Eqs. (72) and (85) it is possible to reach the following expression:

$$\sin(k_2\, l_z) = 0 \tag{86}$$

This is true for the following values of k_2:

$$k_2 = \frac{n\,\pi}{l_z} \tag{87}$$

Thus, considering Eqs. (79) and (87), λ can be determined as

$$\lambda = -\frac{a_s^2}{4D_z} - \frac{D_z n^2 \pi^2}{l_z^2} \tag{88}$$

Last, $u(z)$ can be described using Eqs. (85) and (87), as

$$u(z) = a_1 e^{k_1 z} \sin\left(\frac{n\pi}{l_z}\, z\right) \tag{89}$$

Solution for v(t)

To find a solution for $v(t)$ it is necessary to consider it as a function of the form

$$v(t) = b_1 e^{b_2 t}; \quad b_1,\, b_2 \in \Re \tag{90}$$

Therefore, by combining Eqs. (85) and (75), it can be concluded that the value of b_2 is necessarily equal to

$$b_2 = \lambda \tag{91}$$

Thus, $v(t)$ can be expressed as

$$v(t) = b_1 e^{\lambda t} \tag{92}$$

To find $g(z,t)$ it is necessary to multiply $u(z)$ and $v(t)$, such as

$$g(z,t) = C_n\, e^{\lambda t}\, e^{k_1 z} \sin\left(\frac{n\pi}{l_z} z\right); \qquad C_n \in \Re \tag{93}$$

However, C_n is not yet determined, and the initial condition of Eq. (73) must be used to find this value, as

$$g(z,0) = C_n\, e^{k_1 z} \sin\left(\frac{n\pi}{l_z} z\right) \tag{94}$$

By combining Eqs. (73) and (94), the following expression can be found:

$$C_n \sin\left(\frac{n\pi}{l_z} z\right) = e^{-k_1 z}(\theta_i - \theta_0)\big[H(z) - H(z - b_z)\big] \tag{95}$$

Consequently, the Fourier series that describes the required value for C_n can be defined as

$$C_n = \frac{2}{l_z}\int_0^{l_z} e^{-k_1 z}(\theta_i - \theta_0)\big[H(z) - H(z - b_z)\big] \sin\left(\frac{n\pi}{l_z} z\right) dz \tag{96}$$

By solving the integral of Eq. (96), C_n, the following can be determined:

$$C_n = \frac{4\bar{D}_z e^{-\frac{\bar{a}_s b_z}{2\bar{D}_z}} \left(-2\pi\bar{D}_z n e^{\frac{\bar{a}_s b_z}{2\bar{D}_z}} + \bar{a}_s l_z \sin\left(\frac{\pi b_z n}{l_z}\right) + 2\pi\bar{D}_z n \cos\left(\frac{\pi b_z n}{l_z}\right)\right)}{\bar{a}_s^2 l_z^2 + 4\pi^2 \bar{D}_z^2 n^2} \tag{97}$$

Having obtained all functions that compose θ_h, the homogeneous solution can be described as

$$\theta_h(x,y,z,t) = \frac{(\theta_i-\theta_0)}{4}\left[\operatorname{erf}\left(\frac{b_x-x}{\sqrt{4\,\pi\,t}}\right)+\operatorname{erf}\left(\frac{b_x+x}{\sqrt{4\,\pi\,t}}\right)\right] \times\left[\operatorname{erf}\left(\frac{b_y-y}{\sqrt{4\,\pi\,t}}\right)+\operatorname{erf}\left(\frac{b_y+y}{\sqrt{4\,\pi\,t}}\right)\right]\sum_{n=1}^{\infty}C_n\,e^{\lambda t}\,e^{k_1 z}\,\sin\left(\frac{n\pi}{l_z}z\right) \tag{98}$$

Finally, to obtain the solution of θ, the homogeneous and steady-state solutions must be added together [Eqs. (98) and (26)], as follows:

$$\theta(x,y,z,t) = \theta_0+\frac{(\theta_i-\theta_0)}{4}\left[\operatorname{erf}\left(\frac{b_x-x}{\sqrt{4\pi\bar{D}_x t}}\right)+\operatorname{erf}\left(\frac{b_x+x}{\sqrt{4\pi\bar{D}_x t}}\right)\right] \times\left[\operatorname{erf}\left(\frac{b_y-y}{\sqrt{4\pi\bar{D}_y t}}\right)+\operatorname{erf}\left(\frac{b_y+y}{\sqrt{4\pi\bar{D}_y t}}\right)\right] \times\sum_{n=1}^{\infty}\left\{C_n\,e^{\lambda t}\,e^{k_1 z}\,\sin\left(\frac{n\pi}{l_z}z\right)\right\} \tag{99}$$

Acknowledgments

The authors acknowledge the support provided by the following institutions: the National Council for Scientific and Technological Development (CNPq Grant 304721/2017-4), the Support Research of the Federal District Foundation (FAP-DF Grants 0193.001563/2017 and 0193.002014/2017-68), the Coordination for the Improvement of Higher Level Personnel (CAPES), the National Science Foundation (CMMI Grant 1335456), the University of Brasilia, and the University of Texas at Austin for funding this research.

References

Arairo, W., F. Prunier, I. Djeran-Maigre, and F. Darve. 2012. "A new insight into modelling the behaviour of unsaturated soils." *Int. J. Numer. Anal. Meth. Geomech.* 37 (16): 2629–2645. https://doi.org/10.1002/nag.2151.

Basha, H. A. 1999. "Multidimensional linearized nonsteady infiltration with prescribed boundary conditions at the soil surface." *Water Resour. Res.* 35 (1): 75–83. https://doi.org/10.1029/1998WR900015.

Bharati, V., V. Singh, A. Sanskrityayn, and N. Kumar. 2017. "Analytical solution of advection-dispersion equation with spatially dependent dispersivity." *J. Eng. Mech.* 143 (11): 04017126. https://doi.org/10.1061/(ASCE)EM.1943-7889.0001346.

Brooks, R. H., and A. T. Corey. 1964. *Hydraulic properties of porous media.* Fort Collins, CO: Colorado State Univ.

Cavalcante, A., and J. Zornberg. 2017a. "Efficient approach to solving transient unsaturated flow problems. I: Analytical solutions." *Int. J. Geomech.* 17 (7): 04017013. https://doi.org/10.1061/(ASCE)GM.1943-5622.0000875.

Cavalcante, A., and J. Zornberg. 2017b. "Efficient approach to solving transient unsaturated flow problems. II: Numerical solutions." *Int. J. Geomech.* 17 (7): 04017014. https://doi.org/10.1061/(ASCE)GM.1943-5622.0000876.

Chen, J.-M., Y.-C. Tan, and C.-H. Chen. 2003. "Analytical solutions of one-dimensional infiltration before and after ponding." *Hydrol. Processes* 17 (4): 815–822. https://doi.org/10.1002/hyp.1202.

Chen, J. S., and C. W. Liu. 2011. "Generalized analytical solution for advection–dispersion equation in finite spatial domain with arbitrary time-dependent inlet boundary condition." *Hydrol. Earth Syst. Sci.* 15 (8): 2471–2479. https://doi.org/10.5194/hess-15-2471-2011.

De Luca, D., and J. Cepeda. 2016. "Procedure to obtain analytical solutions of one-dimensional Richards' equation for infiltration in two-layered soils." *J. Hydrol. Eng.* 21 (7): 04016018. https://doi.org/10.1061/(ASCE)HE.1943-5584.0001356.

Fredlund, D. G., and A. Xing. 1994. "Equations for the soil-water characteristic curve." *Can. Geotech. J.* 31 (4): 521–532. https://doi.org/10.1139/t94-061.

Gardner, W. R. 1958. "Some steady-state solutions of the unsaturated moisture flow equation with application to evaporation from a water table." *Soil Sci.* 85 (4): 228–232. https://doi.org/10.1097/00010694-195804000-00006.

Guerrero, J. P., L. C. G. Pimentel, and T. H. Skaggs. 2013. "Analytical solution for the advection–dispersion transport equation in layered media." *Int. Heat Mass Transfer* 56 (1–2): 274–282. https://doi.org/10.1016/j.ijheatmasstransfer.2012.09.011.

Massabó, M., R. Cianci, and O. Paladino. 2011. "An analytical solution of the advection dispersion equation in a bounded domain and its application to laboratory experiments." *J. Appl. Math.* 2011: 493014. https://doi.org/10.1155/2011/493014.

Ozelim, L. and A. Cavalcante. 2013. "Integral and closed-form analytical solutions to the transport contaminant equation considering 3D advection and dispersion." *Int. J. Geomech.* 13 (5): 686–691. https://doi.org/10.1061/(ASCE)GM.1943-5622.0000245.

van Genuchten, M. T. 1980. "A closed-form equation for predicting the hydraulic conductivity of unsaturated soils." *Soil Sci. Am. J. Abstr.* 44 (5): 892–898. https://doi.org/10.2136/sssaj1980.03615995004400050002x.

Wang, Q. J., and J. C. I. Dooge. 1994. "Limiting cases of water fluxes at the land surface." *J. Hydrol.* 155 (3–4): 429–440. https://doi.org/10.1016/0022-1694(94)90181-3.

Warrick, A. W., A. Islas, and D. O. Lomen. 1991. "An analytical solution to Richards' equation for time-varying infiltration." *Water Resour. Res.* 27 (5): 763–766. https://doi.org/10.1029/91WR00310.